

The Physics of Flames in Type Ia Supernovae

M. Zingale¹, S. E. Woosley¹, J. B. Bell², M. S. Day²,
C. A. Rendleman²

¹ Department of Astronomy and Astrophysics, University of California, Santa Cruz, Santa Cruz, CA 95064

² Center for Computational Science and Engineering, Lawrence Berkeley National Laboratory, Berkeley, CA 94720

E-mail: zingale@ucolick.org

Abstract.

We extend a low Mach number hydrodynamics method developed for terrestrial combustion, to the study of thermonuclear flames in Type Ia supernovae. We discuss the differences between 2-D and 3-D Rayleigh-Taylor unstable flame simulations, and give detailed diagnostics on the turbulence, showing that the kinetic energy power spectrum obeys Bolgiano-Obukhov statistics in 2-D, but Kolmogorov statistics in 3-D. Preliminary results from 3-D reacting bubble calculations are shown, and their implications for ignition are discussed.

1. Introduction

Type Ia supernova (SNe Ia) are believed to result from the thermonuclear explosion of a Chandrasekhar mass white dwarf. A thermonuclear flame, born at or near the center of the white dwarf must accelerate tremendously, approaching the speed of sound, in order to account for observational constraints. Uncertainties remain at all stages of the process, from how it ignites, to how the flame accelerates, to whether it may at some point transition to a detonation (see [1] for a review). Speculation on the latter has suggested [2, 3] that the optimal conditions for a transition to detonation to occur are when the flame enters the distributed burning regime, at densities of $\sim 10^7$ g cm⁻³, although other mechanisms have recently been proposed [4].

The range of relevant length scales in the white dwarf is enormous—from the 10^8 cm radius of the white dwarf down to the 10^{-4} – 10^1 cm thickness of the flame. No single simulation can encompass all length scales, so approximations must be made. Large scale 3-D simulations (e.g. [5, 6]) put the entire star on the grid and resolve scales down to $\sim 10^5$ cm, and use a subgrid model to describe the physics of the turbulent burning on the small scales. We have chosen to take a complimentary approach, investigating the physics of turbulent thermonuclear burning on the flame scales, with the hope to use what we've learned to push up to large scales.

Over the last few years, as part of a collaboration between the SciDAC Supernova Science Center at UCSC and the Center for Computational Science and Engineering at LBL, we've introduced a low Mach number model for simulating thermonuclear flames in SNe Ia [7]. In the low Mach number limit, the pressure is decomposed into a thermodynamic component, p_0 , and an $\mathcal{O}(M^2)$ dynamic component, π . This leads to the set of low Mach number thermonuclear

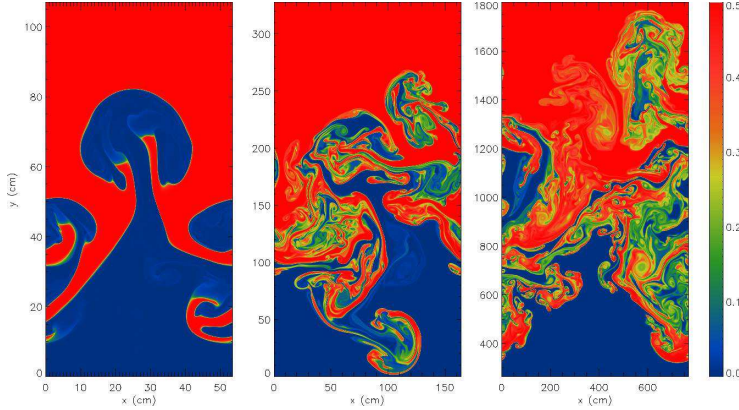


Figure 1. 2-D RT unstable carbon flames at $1.5 \times 10^7 \text{ g cm}^{-3}$ (left), 10^7 g cm^{-3} (middle), and $6.67 \times 10^6 \text{ g cm}^{-3}$ (right), showing the carbon mass fraction. As the density decreases, RT dominates over the burning and we enter the distributed burning regime [9].

flame equations

$$\begin{aligned} \frac{\partial(\rho U)}{\partial t} + \nabla \cdot (\rho U U) &= -\nabla \pi + \rho \vec{g} , \\ \frac{\partial(\rho h)}{\partial t} + \nabla \cdot (\rho U h) &= \nabla \cdot (\lambda \nabla T) - \sum_k \rho q_k \dot{\omega}_k , \\ \frac{\partial(\rho X_k)}{\partial t} + \nabla \cdot (\rho U X_k) &= \rho \dot{\omega}_k . \end{aligned}$$

where ρ , U , and h are the density, velocity, and enthalpy respectively. The enthalpy is related to the internal energy, e through $h = e + p/\rho$. X_k is the abundance of the k^{th} isotope, with reaction rate $\dot{\omega}_k$ and energy release q_k . T is the temperature and λ is the thermal conductivity. Finally, \vec{g} is the gravitational acceleration. This system is constrained to evolve at constant pressure, p_0 , and differentiating the pressure along particle paths yields an elliptic equation for the velocity:

$$\nabla \cdot U = \frac{1}{\rho \frac{\partial p}{\partial \rho}} \left(\frac{1}{\rho c_p} \frac{\partial p}{\partial T} \left(\nabla \cdot \lambda \nabla T - \sum_k \rho \left(q_k + \frac{\partial h}{\partial X_k} \right) \dot{\omega}_k \right) + \sum_k \frac{\partial p}{\partial X_k} \dot{\omega}_k \right). \quad (1)$$

This system filters out sound waves, allowing for much larger timesteps than a compressible code. Eq. (1) is similar to the incompressible constraint, with sources representing thermal diffusion and energy generation across the flame. The solution method is based on second-order projection methods for incompressible flow, embedded in an adaptive mesh refinement framework. Further details of our derivation of the low Mach number model for nuclear flames are given in [7].

2. Results

We have applied this numerical model to several multidimensional studies of thermonuclear flame propagation in SNe Ia [8, 9, 10]. Our approach to date has been to resolve the thermal structure of the flame numerically, eliminating the need for a flame model. The propagation of the flame is entirely determined by the input physics (reaction rate, conductivity) and the flow field. This constrains the regimes we can study however, as we need to have both the flame thickness resolved and several unstable wavelengths contained on our grid.

2.1. Rayleigh-Taylor generated turbulence

Fig. 1 shows 2-D Rayleigh-Taylor (RT) unstable flames at three different densities [9]. At the highest density, the reactions proceed quickly, suppressing the RT instability on the small scales. At the low density end, the small modes of the RT instability grow quickly, and the reactions are

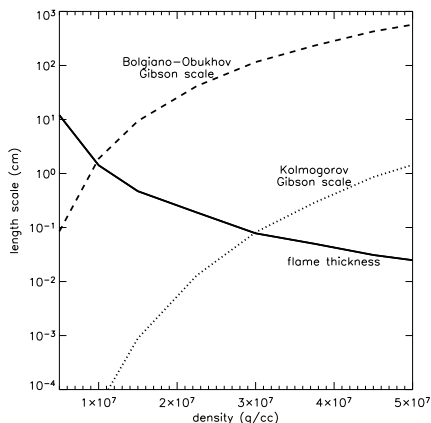


Figure 2. Turbulent flame properties in the supernova. Shown are the flame thickness (solid), the Gibson scale assuming Kolmogorov scaling (dotted line), and the Gibson scale assuming BO statistics (dashed line). The transition to distributed burning, when the Gibson scale is less than the flame thickness, is smaller for BO scaling than for Kolmogorov scaling, as first discussed in [11]. The flame parameters for this figure were computed with the low Mach number algorithm discussed above and a single, screened $^{12}\text{C} + ^{12}\text{C}$ reaction rate.

unable to burn them away. Here, modes smaller than even the flame thickness itself are unstable, and a large mixed region of fuel and ash appears. This is the beginning of the distributed burning regime. In all cases, the RT instability greatly wrinkles the flame, creating more surface area, and dramatically accelerating the flame.

The nature of the turbulence cascading down to the flame scale will directly affect the density at which we enter the distributed burning regime. It was argued that the RT instability would lead to a potential energy cascade, and that Bolgiano-Obukhov (BO) statistics ($u(l) = u'(l/L)^{3/5}$) should be used [11], leading to a lower transition density than Kolmogorov statistics ($u(l) = u'(l/L)^{1/3}$). Fig. 2 illustrates this by computing the Gibson scale for both statistics as a function of density—this is the scale at which the flame can burn away a turbulent eddy before it can turnover. Here we have assumed that the integral scale, L , is 10^6 cm and the turbulent velocity on that scale, u' , is 10^7 cm s $^{-1}$, consistent with the numbers presented in [3]. If the transition is at a lower density, as dictated by BO scaling, it was suggested that a deflagration-detonation transition (DDT) initiated in the distributed burning regime would be more difficult [11], due to the density sensitivity of the carbon reaction rates. Our 2-D RT studies [9] also suggest that a DDT is not possible. The true nature of the turbulent cascade can be determined through resolved flame simulations.

We studied a 3-D RT unstable flame in detail [10], and found that after the linear growth, turbulence dominates the dynamics. Fig. 3 shows a volume rendering of the carbon mass fraction and the associated kinetic energy power spectrum. We see that it is a Kolmogorov power spectrum, not BO, as previously suggested [11]. Gravity creates a preferred direction in the domain, and the turbulence is strongly anisotropic on the large scales. However, on the small scales, the turbulence becomes more and more isotropic, as determined by looking at isosurfaces of the Fourier transform of the turbulent kinetic energy in \mathbf{k} -space [10].

Recent analytic work [12] argued that BO statistics should only apply in 2-D. Fig. 3 also shows a 2-D reactive RT instability, and the power spectrum shows a clear $-11/5$ scaling over more than a decade in wavenumber. It is essential to use a large domain, with many unstable modes to see this scaling in 2-D—this 2-D simulation is effectively 2048×4096 zones. This comparison between 2-D and 3-D confirms the assertions in [12], and therefore, for SNe Ia, 3-D turbulence models should assume Kolmogorov scaling, not BO. With this dimensionality dependence, together with Fig. 2, we can understand why our 2-D study [9] showed a lower transition density to distributed burning than our corresponding 3-D RT flame [10]. This difference in RT generated turbulence demands that any SNe Ia simulations be run in 3-D, since turbulence acts on all scales of the problem. Since the transition density is higher with Kolmogorov turbulence, it may be easier to ignite a detonation than our 2-D estimates [9] have suggested. Studies of flames interacting with Kolmogorov turbulence in 3-D are underway, and

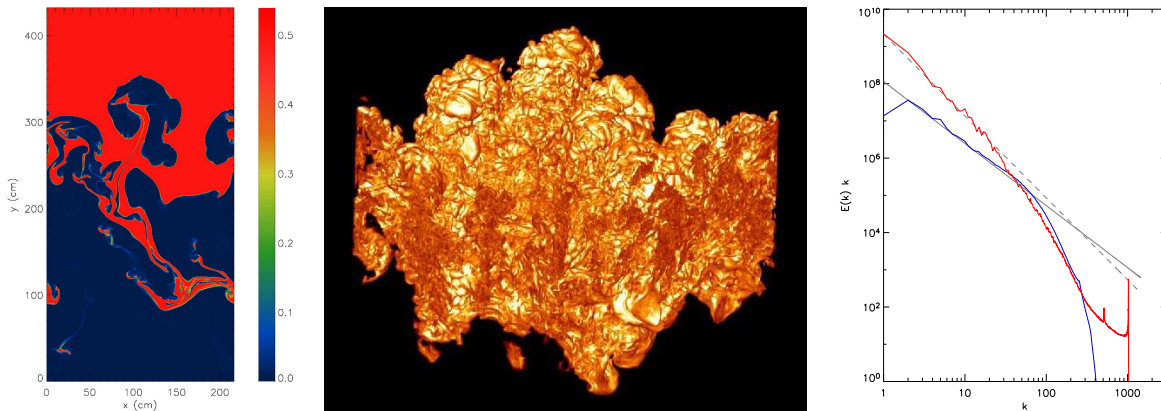


Figure 3. 2-D (left) and 3-D [10] (center) RT unstable carbon flame at $1.5 \times 10^7 \text{ g cm}^{-3}$. The kinetic energy power spectrum (right) shows the 3-D flame (blue line) following a $-5/3$ power law (gray solid) and the 2-D flame (red line) following a $-11/5$ power law (gray dashed). The 2-D simulation was run in a large domain (216 cm wide vs. 53.5 cm wide for the 3-D), necessary to see the scaling trend. This wider domain accounts for the higher peak kinetic energy.

will allow us to explore more fully whether a transition to detonation is possible.

2.2. Bubbles

Finally, we consider an alternate configuration from the flame sheets that we have been studying, a burning bubble. The ignition of an SNe Ia likely begins with one or many hotspots that begin to burn faster than they can cool by expansion. These bubbles are buoyant and rise as they grow, possibly merging as they consume the carbon fuel in the star. The drag force on a rising bubble is smaller than that on a sheet, so we would expect different dynamics to ensue. Of particular interest is the small scale structure that develops on the bubble. The exploding white dwarf has an extremely large Reynolds number, so we expect turbulence to dominant early in the evolution of the reacting bubble. It is possible that this turbulence will shed sparks from the bubble as it rises, and if these are small enough, they can be entrained in the ambient flow instead of buoyantly rising on their own, igniting the star in new regions.

Fig. 4 shows the preliminary results of a burning rising bubble. This was again done at a density of $1.5 \times 10^7 \text{ g cm}^{-3}$, far from the conditions of ignition, but approachable by DNS calculations. The general features of the evolution should be qualitatively the same as those of a bubble near ignition conditions. This is an exceptionally large calculation, corresponding to a $2048 \times 2048 \times 3072$ zone effective grid. At present, over 200 million zones are carried, and this calculation is still in progress. As the figure shows, at late times, a hole develops in the center of the bubble, due to the strong shear at the top of the bubble, which suppresses the burning. At higher densities, the faster reaction rate may suppress this hole formation. Also apparent is the growth of small scale structure on the sides of the bubble, driven by shear. This is only seen in high resolution 3-D studies of reacting bubbles. Large scale simulations employing flame models would likely wash this structure away, preventing the shedding of sparks, and perhaps missing a key component of the ignition process. More studies of resolved burning rising bubbles at high Reynolds number are needed to determine how large of an effect this spark shedding may be.

3. Summary

We presented results from a program of study of small-scale flame physics. We showed that in 3-D, the turbulent cascade obeys Kolmogorov scaling while in 2-D, BO scaling is observed. This difference in turbulence scaling demands that SNe Ia simulations be run in 3-D. It is interesting

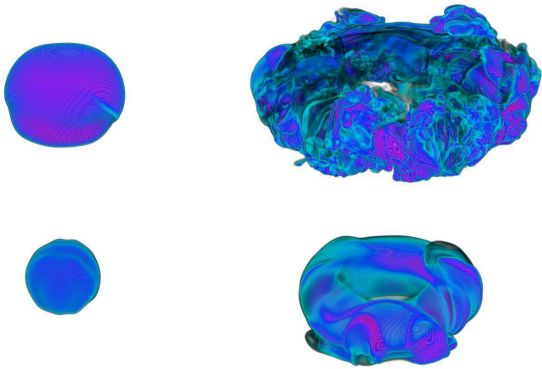


Figure 4. 3-D simulation of a buoyant rising bubble at $1.5 \times 10^7 \text{ g cm}^{-3}$, at four different times. The reactions are slow enough at this density that the initially spherical bubble deforms into a torus due to shear at the top. At late times, the bubble is becoming turbulent, with lots of small scale structure appearing.

to note that the Sharp-Wheeler model for RT [13] predicts a speed, $u \sim l^{1/2}$, between BO and Kolmogorov scaling. Flame models using different assumptions of the turbulence speed on small scales will lead to differing results. If large scale simulations accurately capture the turbulent cascade for more than a decade in wavenumber, then it is a good approximation that the turbulence fed into the subgrid model is Kolmogorov and isotropic.

Of critical importance to understanding the early stages of the explosion is the dynamics of reacting bubbles. Resolved calculations are very difficult, but can have enormous consequences. If the bubbles quickly become turbulent, as expected in the high Reynolds number flow in the white dwarf, then it is likely that sparks will be shed and advect with the background convective motions to ignite other regions of the star. This may make multipoint, time-dependent ignition an essential ingredient in the explosion process.

Current work involves extending our low Mach number model to accommodate multiple scale heights. This would allow for full star calculations, while retaining the ability to take timesteps restricted by only the fluid velocity rather than the sound speed. This would be ideal for studies of the ignition process itself, and allow for the evolution to continue directly into the explosion phase. These large scale simulation will be the focus of the next years of our collaboration.

Acknowledgments

Support for this work was provided by DOE grant No. DE-FC02-01ER41176 to the Supernova Science Center/UCSC and the Applied Mathematics Program of the DOE Office of Mathematics, Information, and Computational Sciences under contract No. DE-AC03-76SF00098. Work presented used the NERSC seaborg, ORNL cheetah, and the NASA Ames Columbia machines.

References

- [1] W. Hillebrandt and J. C. Niemeyer. *Annu Rev Astron Astrophys*, 38:191–230, 2000.
- [2] A. M. Khokhlov. *Astron Astrophys*, 245:114–128, 1991.
- [3] J. C. Niemeyer and S. E. Woosley. *Astrophys J*, 475:740–753, 1997.
- [4] T. Plewa, A. C. Calder, and D. Q. Lamb. *Astrophys J*, 612:L37–L40, 2004.
- [5] F. K. Röpkke and W. Hillebrandt. *Astron Astrophys*, 431:635–645, 2005.
- [6] V. N. Gamezo, A. M. Khokhlov, E. S. Oran, A. Y. Chtchelkanova, and R. O. Rosenberg. *Science*, 299:77–81, 2003.
- [7] J. B. Bell, M. S. Day, C. A. Rendleman, S. E. Woosley, and M. A. Zingale. *J Comput Phys*, 195(2):677–694, 2004.
- [8] J. B. Bell, M. S. Day, C. A. Rendleman, S. E. Woosley, and M. Zingale. *Astrophys J*, 606:1029–1038, 2004.
- [9] J. B. Bell, M. S. Day, C. A. Rendleman, S. E. Woosley, and M. Zingale. *Astrophys J*, 608:883–906, 2004.
- [10] M. Zingale, S. E. Woosley, C. A. Rendleman, M. S. Day, and J. B. Bell. *Astrophys J*, 2005. accepted.
- [11] J. C. Niemeyer and A. R. Kerstein. *New Astron*, 2:239–244, 1997.
- [12] M. Chertkov. *Phys Rev Letters*, 91(11):115001, 2003.
- [13] D. H. Sharp. *Physica*, 12D:3–18, 1984.